

Supporting Information

for

**The Energy Blocker Inside The Power House: Mitochondria
Targeted Delivery Of 3-Bromopyruvate**

Sean Marrache^a and Shanta Dhar^{a,b,c,}*

^aNanoTherapeutics Research Laboratory, Department of Chemistry, University of Georgia, Athens, GA 30602

^bDepartment of Physiology and Pharmacology, University of Georgia, Athens, GA 30602

^cRegenerative Bioscience Center, University of Georgia, 425 River Road, Athens, GA 30602

*Address correspondence to shanta@uga.edu

Materials and Instrumentations.

All chemicals were received and used without further purification unless otherwise noted. Dicyclohexylcarbodiimide (DCC), 6-bromohexanoic acid, 4-dimethylaminopyridine (DMAP), NaBH₄, and (3-(4,5-dimethylthiazol-2-yl)-2,5-diphenyltetrazolium bromide (MTT), adenosine 5'-triphosphate (ATP) disodium salt hydrate, gold(III) chloride trihydrate (HAuCl₄·3H₂O), 30% hydrogen peroxide (H₂O₂), and etoposide were purchased from Sigma-Aldrich. 3-Bromopyruvic acid (3-BP) hydrate was purchased from Acros Organics. SH-polyethyleneglycol-NH₂ (SH-PEG-NH₂) of molecular weight of 3500 was obtained from JenKem Technology, USA. Potassium iodide (KI), Ethyl(dimethylaminopropyl) carbodiimide (EDC) and *N*-hydroxysuccinimide (NHS) were procured from Sigma-Aldrich. Spectra/Por® Dialysis membranes with a molecular weight cutoff of 5000 and 2000 Da were purchased from Spectrum® Labs. Alexa Fluor® 488 Annexin V/Dead cell apoptosis kit was purchased from Invitrogen. Lactate assay kit was obtained from BioVision, CA, USA. CellTiter-Glo® luminescent cell viability assay kit from Promega was used to quantify cellular ATP content. The Ambion® KDaAlert™ Glyceraldehyde 3-phosphate dehydrogenase (GAPDH) assay kit was purchased from Life Technologies. Interleukin (IL)-6 and tumor necrosis factor (TNF)-α cytokines were tested using BD OptEIA mouse enzyme-linked immunosorbent assay (ELISA) kits. Ultra-pure lipopolysaccharide (LPS) was purchased from Invivogen, CA, USA. Bicinchoninic acid (BCA) protein assay kit (Pierce 23227) was purchased from Thermo Scientific. Human hexokinase 2 (HK2) was procured from Sigma-Aldrich (Catalogue number: H2917-10UG). The mitochondrial isolation kit for mammalian cells was purchased from Thermo Scientific. Mesenchymal stem cell basal medium

recombinant human fibroblast growth factor-basic, recombinant human fibroblast growth factor-acidic, and recombinant human epithelial growth factor were purchased from ATCC.

Distilled water was purified by passage through a Millipore Milli-Q Biocel water purification system (18.2 M Ω) containing a 0.22 μ m filter. ^1H , ^{13}C spectra were recorded on a 400 MHz Varian NMR spectrometer. ^{31}P NMR spectrum was recorded on a 500 MHz Varian NMR spectrometer using phosphoric acid as a standard. Dynamic light scattering (DLS) measurements were carried out using a Malvern Zetasizer Nano ZS system. Transmission electron microscopy (TEM) images of NPs were taken in a Tecnai 20 FEI microscope. Cellular TEM images were collected on a JEM-1210 Transmission Electron Microscope Equipped with an XR41C Bottom-Mount CCD Camera. Laser irradiation was performed using a Melles Griot 660 nm 56 ICS series diode laser equipped with a fiber optic cable in a dark environment. Optical measurements were carried out on a NanoDrop 2000 spectrophotometer. Flow cytometry studies were performed on a BD LSRII flow cytometer equipped with digital acquisition using FACSDiva v6. Plate reader analysis was performed on a Bio-Tek Synergy HT microplate reader. Bioenergetic assays were carried out using a Seahorse XF24 analyzer (Seahorse Biosciences, North Billerica, MA, USA).

Table S1. Characterization of AuNPs, data presented here is an average of three independent preparations

NP System	Z-Average (nm)	Number Average Diameter (nm)	PDI	Zeta Potential (mV)	% 3-BP Loading	% Coupling Efficiency 3-BP
T-AuNP	19.1 ± 0.8	3.1 ± 0.8	0.38	17.6 ± 1.5	-	-
T-3-BP-AuNP	18.8 ± 0.9	4.3 ± 0.7	0.31	11.0 ± 2.3	23.7 ± 0.5	7.9 ± 0.2
NT-AuNP	27.7 ± 1.1	2.9 ± 0.2	0.39	15.3 ± 0.5	-	-
NT-3-BP-AuNP	26.6 ± 4.4	3.1 ± 0.9	0.19	5.8 ± 0.7	24.3 ± 0.2	8.1 ± 0.1

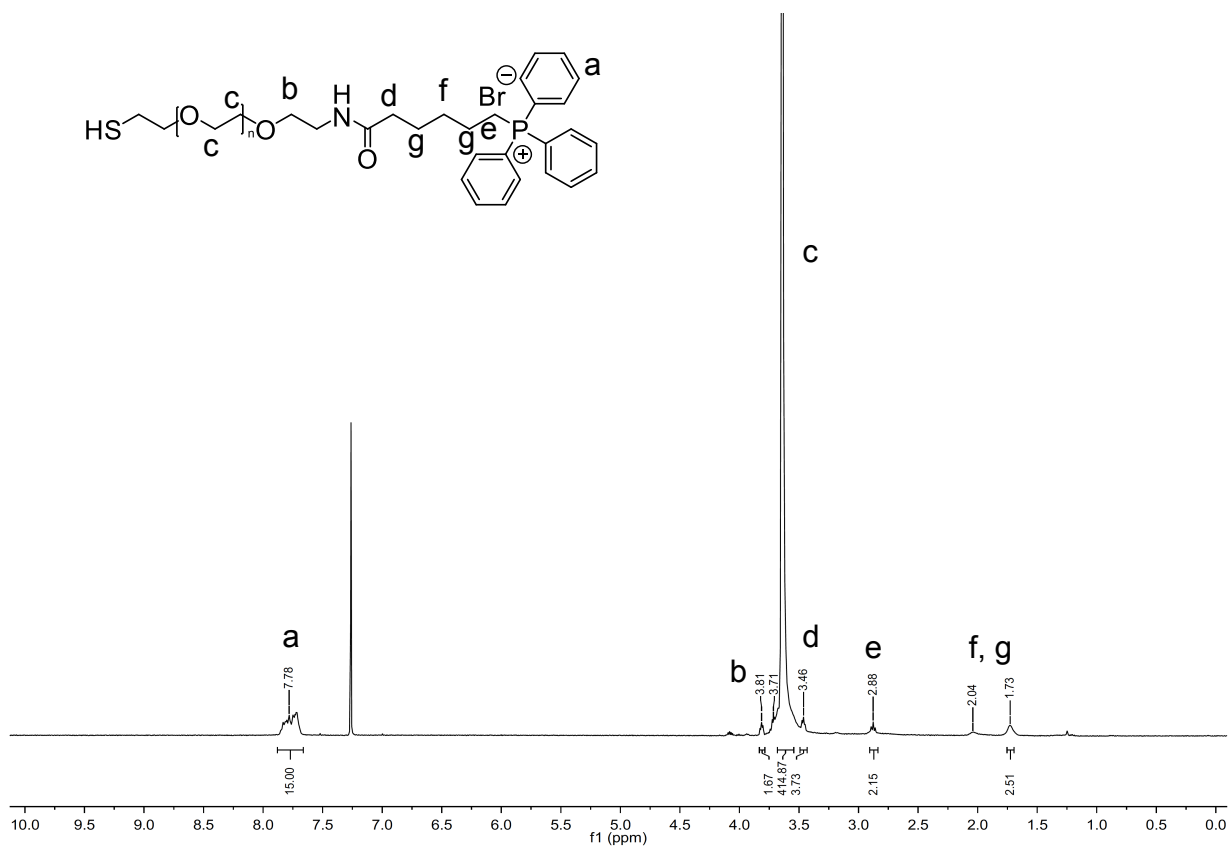


Figure S1. ^1H NMR of TPP-PEG-SH in CDCl_3 .

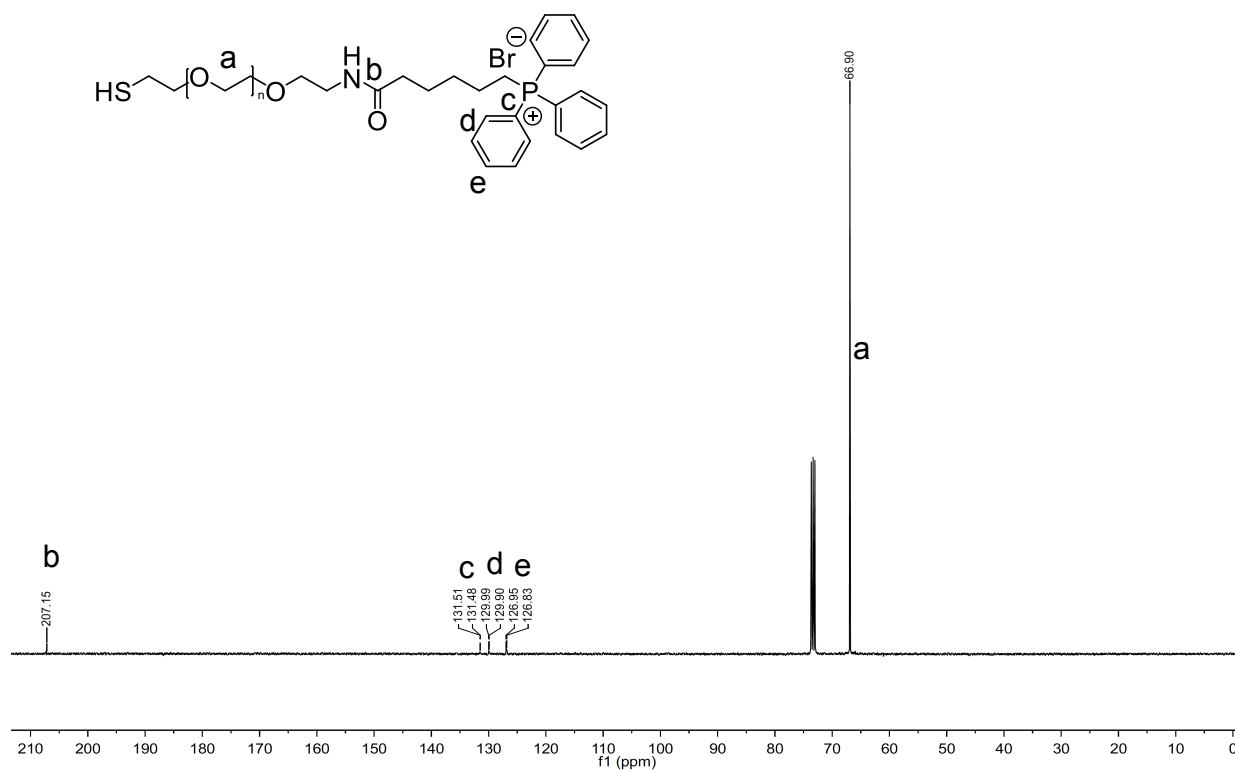


Figure S2. ^{13}C NMR of TPP-PEG-SH in CDCl_3

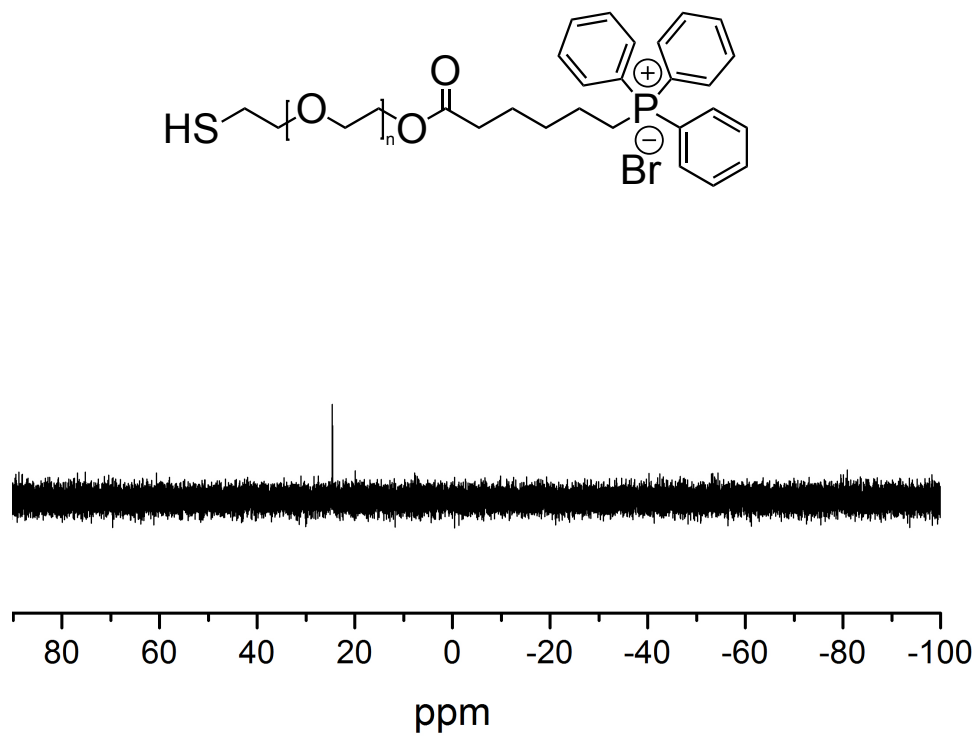


Figure S3. ^{31}P NMR of TPP-PEG-SH in CDCl_3

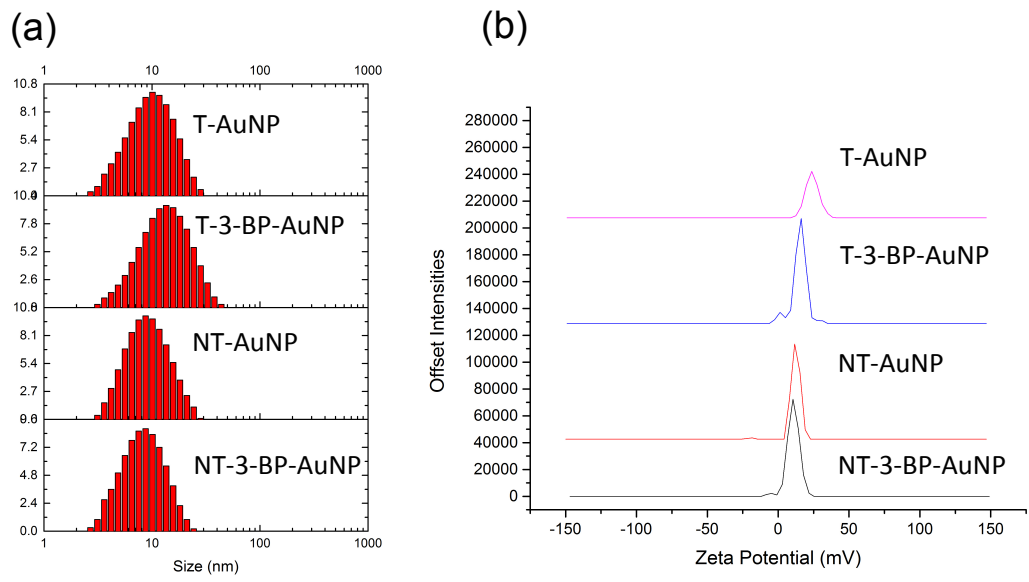


Figure S4. Overlay of DLS plots for hydrodynamic diameter (a) and zeta potential (b) of different NPs.

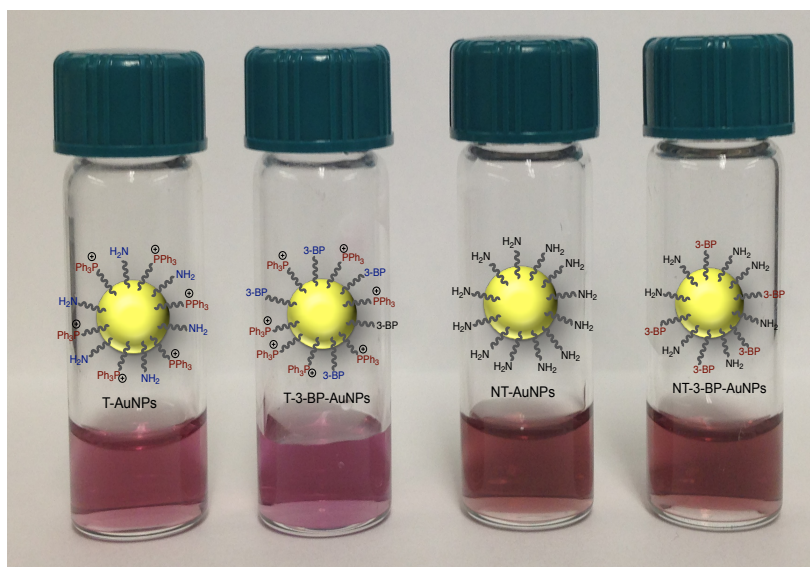


Figure S5. Photographs of T-AuNPs, T-3-BP-AuNPs, NT-AuNPs, and NT-3-BP-AuNPs after resuspension in water.

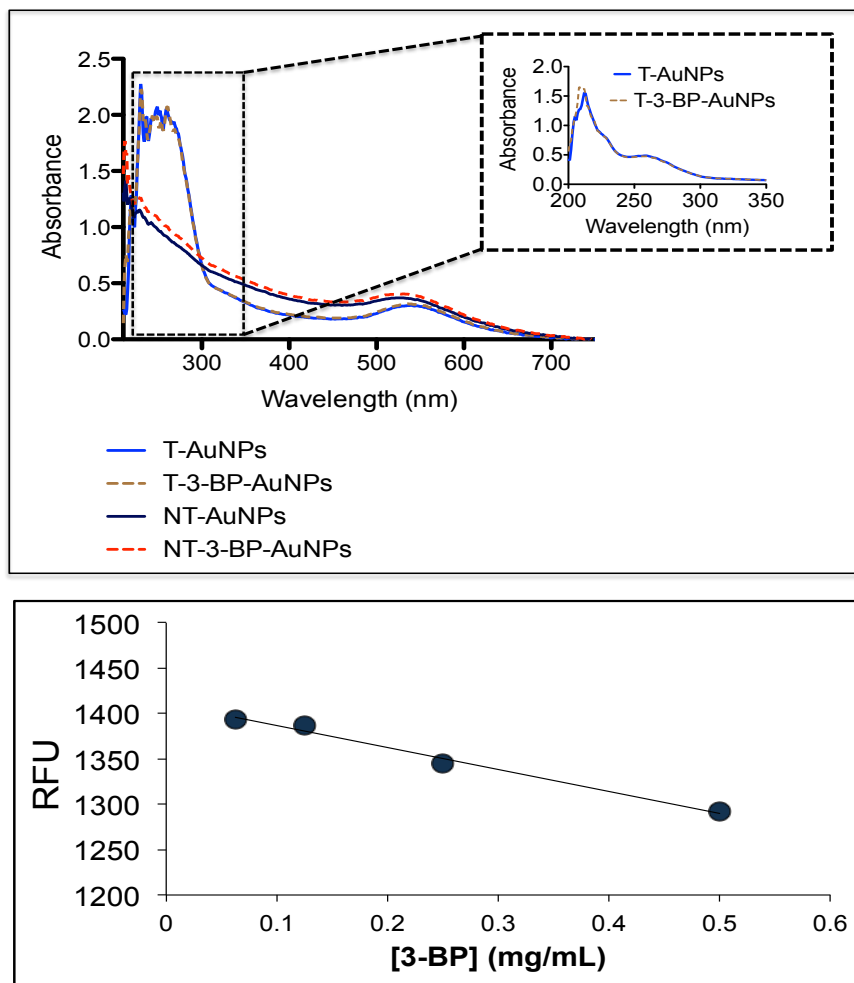


Figure S6. (Top) UV-vis characterization of T and NT-AuNPs showing the absence of any aggregation with inset showing the TPP peaks from T-AuNP. (Bottom) GAPDH standard curve using 3-BP.

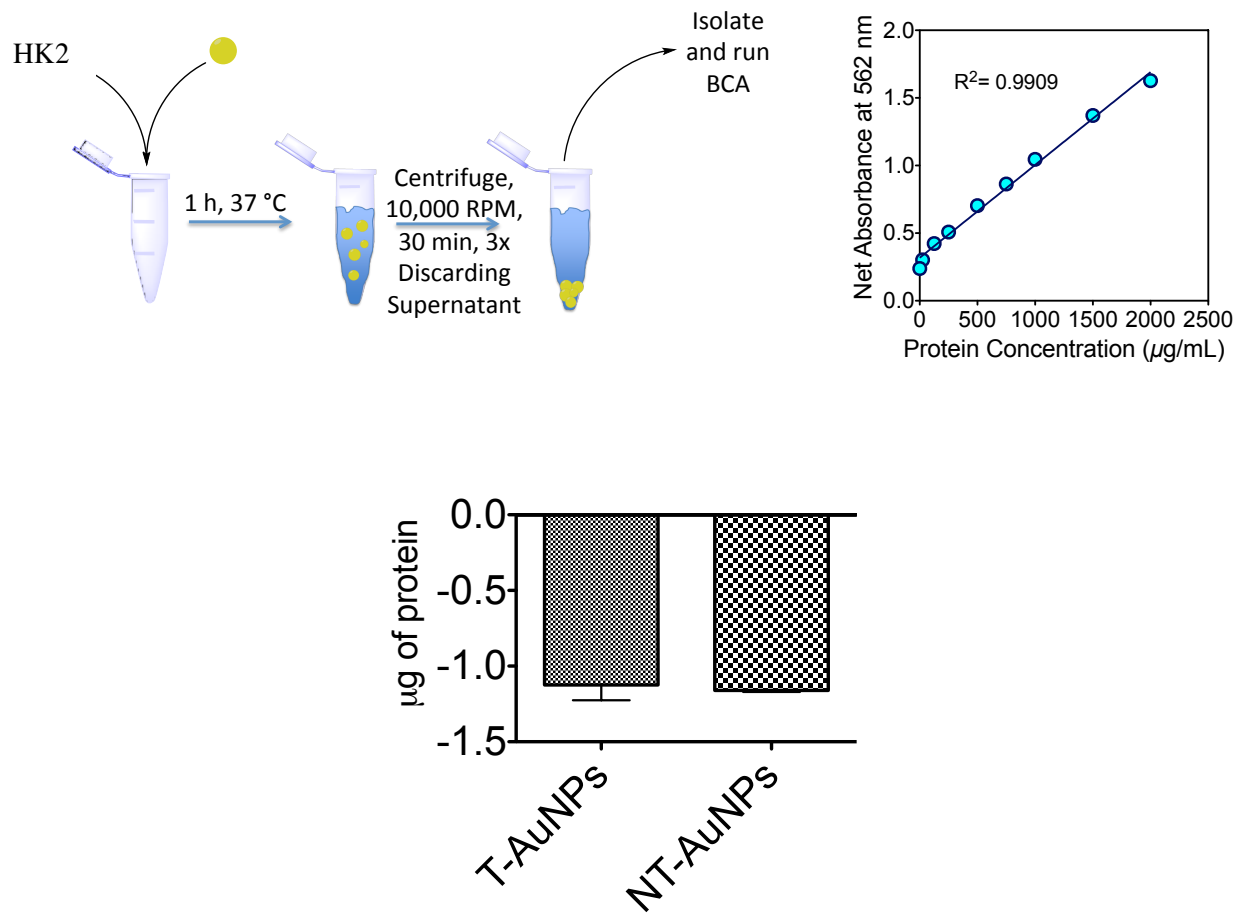


Figure S7. Diagram showing HK2 assay and the BCA standard curve (top). T and NT-AuNPs without any 3-BP do not show HK2 binding (bottom).

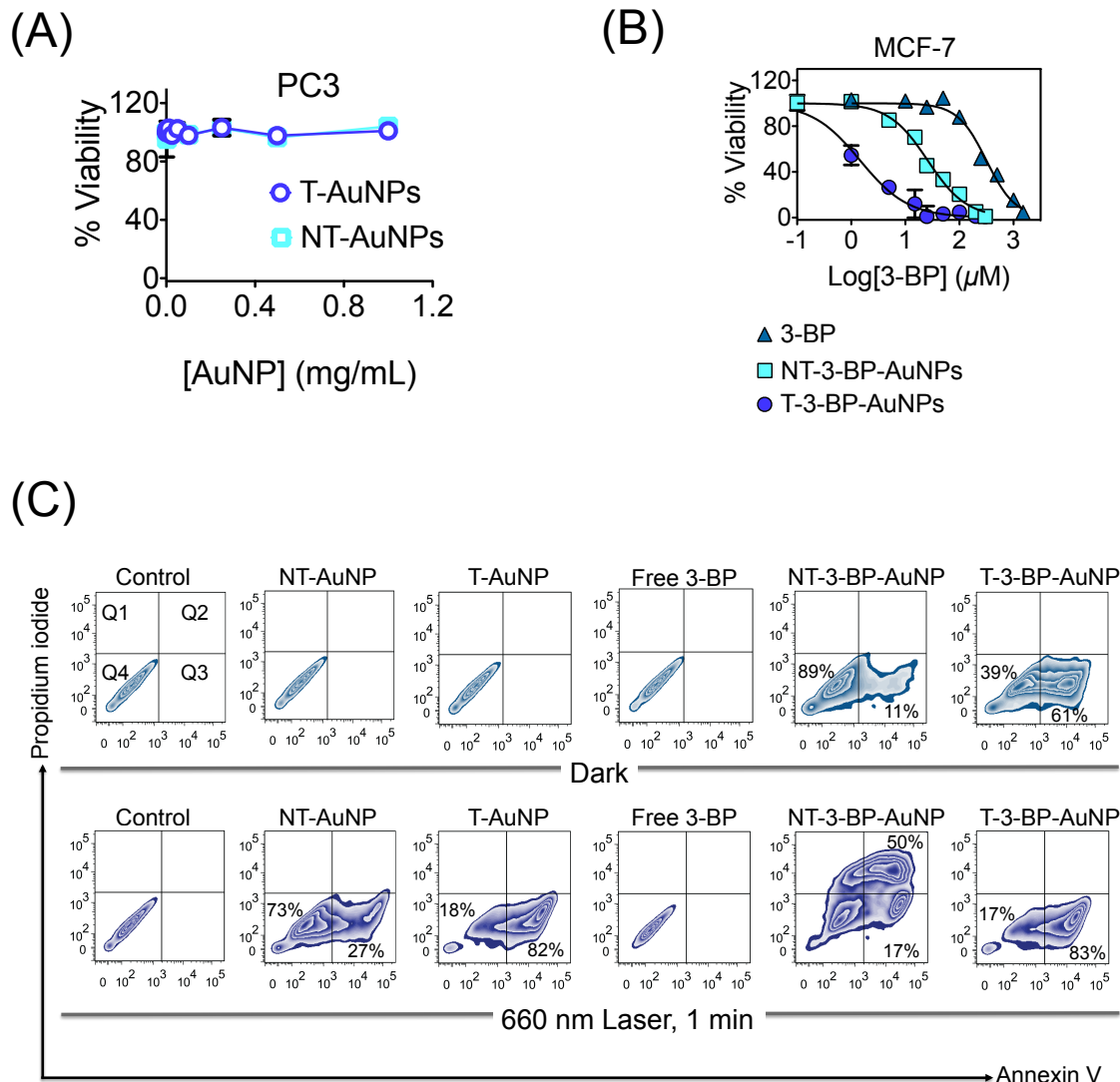


Figure S8. (A) Cell viability in PC3 cells after treatment with T-AuNPs, NT-AuNPs. **(B)** Cell viability in MCF-7 cells after treatment with 3-BP, T-3-BP-AuNPs, and NT-3-BP-AuNPs. Cell viability was assessed by the MTT assay after treatment with the indicated concentrations of the test articles for 72 h. The data are mean \pm SD ($n = 3$ wells). **(C)** (Top) Apoptotic patterns induced in PC3 cells upon treatment with T-AuNP (1 mg/mL), NT-AuNP (1 mg/mL), T-3-BP-AuNP (14.1 μ g/mL with respect to NP, 10 μ M with respect to 3-BP), NT-3-BP-AuNP (13.7 μ g/mL with respect to NP, 10 μ M with respect to 3-BP), free 3-BP (10 μ M) for 6 h at 37 $^{\circ}$ C in the dark. (Bottom) Apoptosis induced in PC3 cells

upon treatment with T-AuNP (1 mg/mL), NT-AuNP (1 mg/mL), T-3-BP-AuNP (14.1 μ g/mL with respect to NP, 10 μ M with respect to 3-BP), NT-3-BP-AuNP (13.7 μ g/mL with respect to NP, 10 μ M with respect to 3-BP), free 3-BP (10 μ M) for 4 h at 37 °C, followed by irradiation with 660 nm laser for 1 min, and further incubation for 12 h. x-axis: Alexa Fluor® 488 Annexin V; y-axis: propidium iodide (PI). Live cells accumulate in Q4 (Annexin V and PI negative), cells undergoing early apoptosis accumulate in Q3 (Annexin V positive and PI negative), cells in end-stage apoptosis or necrotic stage accumulate in Q2 (Annexin V and PI positive).

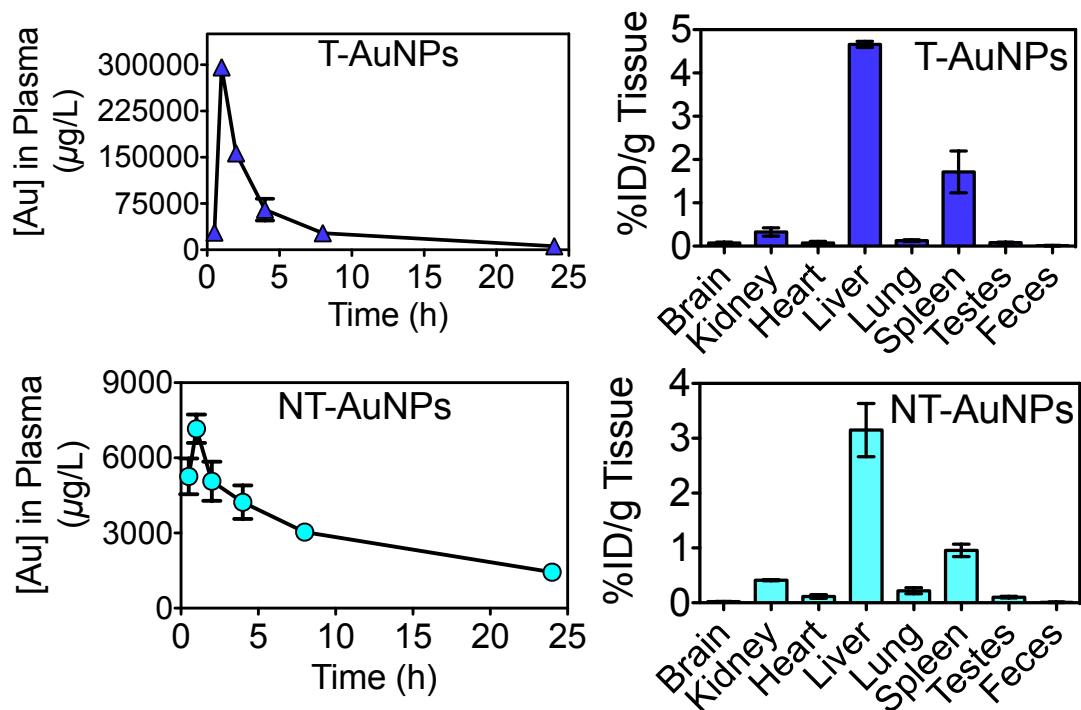


Figure S9. Variation of Au concentration in $\mu\text{g/L}$ in plasma with time and tissue distribution following the administration of T-AuNPs and NT-AuNPs intravenously to male rats.